



Review on Testing Methods for Permeability and Selectivity Measurements of Polymeric Membranes

Yousef Alqaheem*

Petroleum Research Center, Kuwait Institute for Scientific Research, Kuwait

* Corresponding author. Tel.: +965 24956929. Fax: +965 23980445
(E-mail: yqaheem@kisir.edu.kw)

Abstract: Polymeric membranes can provide an energy-saving solution for gas separation. The technology is also compact and easy to maintain, though, for commercial applications, the membrane performance should be conscientiously tested as the data could vary significantly. Unfortunately, there is no standard procedure for evaluating the membranes for gas separation. This paper gives general guidelines on various methods for determining the membrane permeability and selectivity with the commonly used setup. The paper also discusses the measurements and calculations of product purity and gas recovery for better comparison with other separation technologies.

Key Words: Gas-separation membrane, gas permeability, real selectivity, time-lag method, gas recovery

1. Introduction

Polymeric membranes have been commercialized for gas separation since the 1980s [1]. The first application was for the removal of hydrogen from methane by a polysulfone membrane [2]. The applications were then expanded to cover acid gas removal, and oxygen enrichment [3]. The membrane is considered as an environmentally-friendly technology because it operates at low energy and it does not produce toxic wastes [4].

Furthermore, the membrane is easy to scale up and can have a continuous life of five years [5,6].

There are many materials for polymeric membranes and their performance varies broadly depending on the polymer and the gases to be separated. The widely accepted theory for gas transport through dense polymeric membranes is the solution-diffusion

model [7]. The model states that the gas is first absorbed on the membrane surface and then dissolved. The gas then diffuses inside the membrane by a means of free volumes. The gas is then desorbed on the low-pressure side. Their dominant factors that control the

solution-diffusion model are solubility and diffusivity [8]. The permeability (P), which is one of the key parameters to describe the membrane performance, is the product of solubility and diffusivity:

$$P = K_A \times D_A \quad (1)$$

where K_i and D_i are the sorption and diffusion coefficients of gas a , respectively. The permeability gives information about the quantity of the produced gas (also known as the permeate). Experimentally, the permeability can be determined without the need for solubility and diffusivity measurements.

There are typically three approaches to measure the permeability: using a bubble flowmeter, a mass flowmeter, and the time-lag technique. Each method will be discussed in detail in the following sections. The permeability data is given in Barrer (named after Richard Barrer) and it is calculated by:

$$P \text{ (Barrer)} = \frac{V_A \times l}{A \times \Delta P} 10^{10} \quad (2)$$

where V_A is the volume flowrate of the permeate of gas a ($\text{cm}^3 \text{ s}^{-1}$), l is the membrane thickness (cm), A is the active membrane area (cm^2), and ΔP is the pressure difference across the membrane (cmHg). The mentioned techniques for permeability calculations actually measure the volume flowrate which will be used to calculate the permeability as given in equation 2. Because the volume of the gas depends on the pressure and temperature, the volume flowrate for

equation 2 should be stated at STP (standard temperature and pressure of 0°C and 1 atm). STP should not be confused with NTP (normal temperature and pressure) where the temperature is 20°C instead of 0°C . The pressure in NTP is 1 atm which is very close to 1 bar (0.986 atm). Assuming ideal gas behavior, the volume flowrate can be converted from NTP to STP using the following equation:

$$V_{STP} = \frac{T_{STP}}{T_{NTP}} V_{NTP} = \frac{273}{293} V_{NTP} = 0.925 V_{NTP} \quad (3)$$

where T_{STP} and T_{NTP} , are the temperatures of 273 and 293K, respectively. This gives a correction factor of 0.925 when the flowrate is converted of NTP to STP.

case of a symmetric membrane which is made from a single material with a uniform structure (porous or dense). However, for asymmetric membranes made from two or more materials (composite), characterization techniques such as scanning electron microscopy (SEM) are needed to measure the

The membrane thickness in equation 2 is commonly determined using a caliper in the

thickness of the selective material which is usually the dense layer. Other techniques such as transmission electron microscopy (TEM) and atomic force microscopy (AFM)

can be used as well [9]. It is worth mentioning that asymmetric membranes can be made as well from a single material using the phase-inversion method [10].

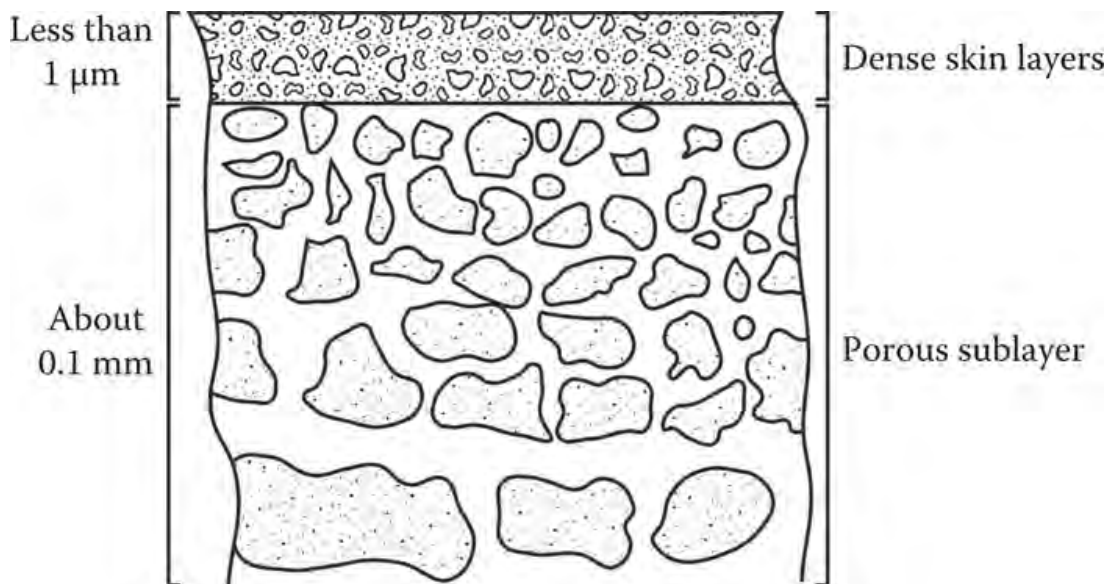


Figure 1. Structure of Asymmetric Membrane Made from One Material by the Phase-inversion Method [12]

The developed membrane will have two structures: porous and dense, as given in Figure 1, despite the use of one material. In this case, the membrane thickness is the skin of the dense layer similar to the composite

membrane [11]. In literature, most of the membranes are made from the phase-inversion method and therefore, a spectroscopy technique is needed to measure the membrane thickness.

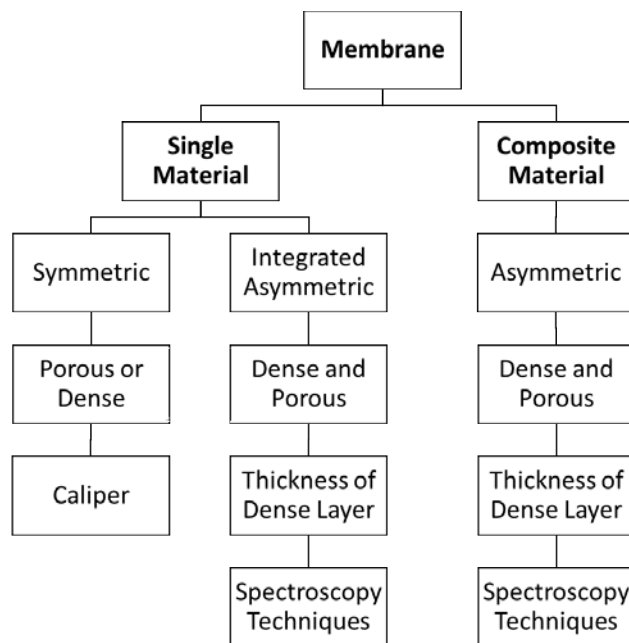


Figure 2. Determination of the Membrane Thickness for the Calculation of Gas Permeability in Barrer

Figure 2 gives general guidelines for determining the membrane thickness for calculating the permeability in Barrer. Sometimes it is difficult to measure the membrane thickness as it can vary notably along with the membrane structure. Furthermore, the spec-

troscopy technique maybe not available to measure the membrane thickness. Thus, a new unit for gas permeability was defined and it is known as permeance (Q). It is calculated similar to equation 2 but without the use of thickness:

$$Q \text{ (GPU)} = \frac{V_A}{A \times \Delta P} 10^6 \quad (4)$$

where V_A , A , and ΔP shares the same units as equation 2. The unit of permeance is the gas permeation unit (GPU).

Unfortunately, the units of Barrer and GPU cannot be converted if the membrane thickness was not stated. If the membrane thickness is known, the following equation can be used to convert the permeability from Barrer to GPU.

$$Q \text{ (GPU)} = \frac{P \text{ (Barrer)}}{10,000 \times l} \quad (5)$$

It should be noted that Barrer is considered as a more accurate unit than GPU for stating the

permeability as it takes into consideration the membrane thickness. This will make the

comparison with other reported data more reliable for the same membrane. However, industrially, the membrane performance is widely described by GPU unit rather than Barrer for easier calculations.

This paper reviews the methods for measuring the permeability in polymeric membranes using different approaches such as bubble flowmeter, mass flowmeter, and the time-lag method (also known as the closed volume technique). The paper also describes

about calculations of solubility and diffusion coefficients. Furthermore, the paper discusses the determination of gas selectivity which represents the purity of the gas produced. The paper also differentiates between the ideal and real selectivities and the latter is a key parameter for determining the membrane performance for commercial applications. The calculations of product purity and gas recovery are also important to evaluate the membranes with other separation technologies such as the amine process.

2. Permeability Measurements

The permeability can be calculated based on the measured flowrate of the permeate. There are extensively three ways to measure membrane permeability: (1) bubble flowmeter, (2) mass flowmeter, and (3) time-lag technique. Before starting the evaluation, the membrane should be examined visually. Any visible holes or defects may cause incorrect value of the permeability. The membrane is then inserted in a cell, usually made of metal housing. Rubber rings (with o-shape) are traditionally employed to seal the membrane and prevent gas leakage. The gas is normally

fed to the membrane by a gas cylinder equipped with a pressure regulator. A mass flow controller (MFC) is commonly used to control the feed flowrate. This device is used to set the volume flowrate of the feed gas. The output gas (after MFC) will be at atmospheric pressure and a pressure control valve can be employed to elevate the pressure. The feed gas will reach the membrane surface and the volume flowrate of the permeate will be measured to determine the permeability. Figure 3 shows the common experimental setup for the permeability test.

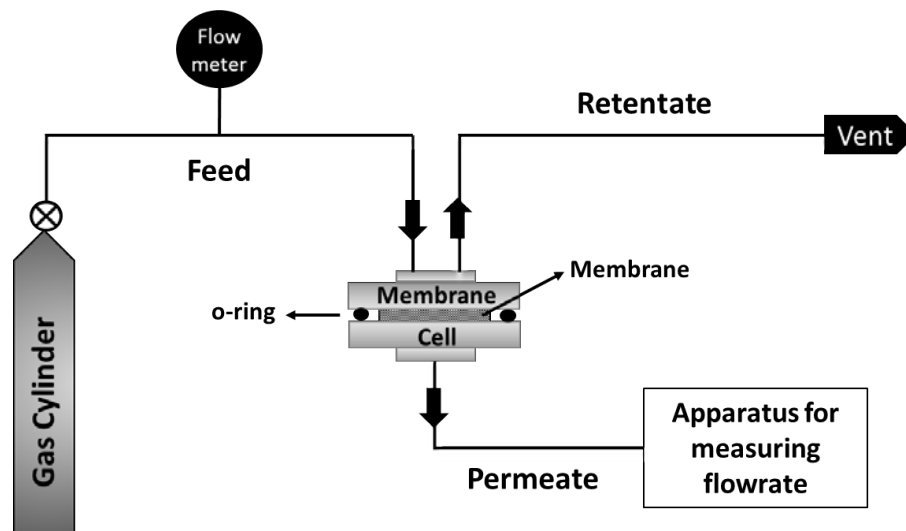


Figure 3. Experimental Setup for Determining the Gas Permeability of Polymeric Membranes

It should be noted that there are some inputs that should be defined before performing the membrane assessment. These inputs will significantly affect the permeability data. The parameters are the gas feed flowrate, temper-

ature, pressure, membrane area, and membrane thickness. The area is calculated based on the cross-section area of the membrane as follows:

$$A = \pi \frac{d^2}{4} \quad (6)$$

where d is the diameter of the exposed area to the gas which is usually lower than the total diameter of the membrane as the o-rings will block some region for sealing.

25–35°C, pressure of 3–10 bar, area of 10–15 cm², membrane thickness of 10–300 μm as given in Table 1. The following sections will discuss the methods for determining the permeability using the bubble flowmeter, mass flowmeter, and the time-lag technique.

Unfortunately, there are no standards for the input parameters, however, the following values are widely used in literature: feed flowrate of 0.1–1 cm³ s⁻¹, temperature of

Table 1. Operating Conditions for Membrane Testing Used by Most Researchers [13-26]

Operating condition	Value
Feed flowrate	0.1 – 1 cm ³ s ⁻¹
Temperature	25 – 35°C
Pressure	3 – 10 bar
Membrane effective area	10 – 15 cm ²
Membrane thickness	10 – 300 μm

Bubble Flowmeter

The bubble flowmeter is considered as the oldest and the most cost-effective technique for measuring the permeability. Broadly, the system is suitable for measuring flowrates between 0.1 to 1000 cm³ s⁻¹. The instrument consists of a graded burette along with a rubber bulb and soap solution. The gas enters the side of the instrument and then the bulb is squeezed to create a soap film that will be lifted by the gas in the form of a bubble. The

burette is marked with a starting point in which a stopwatch will be used to measure the time needed for the bubble to cross the final mark as shown in Figure 4. By dividing the volume by time, the volume flowrate can be determined. The error expected for this instrument is within ±5% [28]. Nevertheless, if the experiment was carried perfectly, the error can be reduced to ±1% [29].

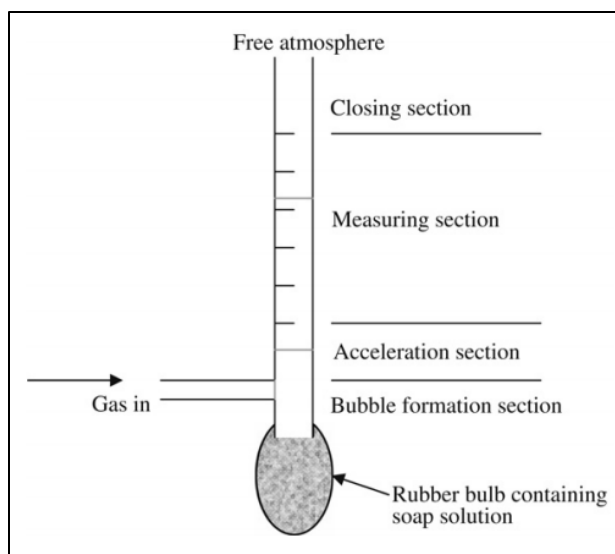


Figure 4. Components of the Bubble Flowmeter for Gas Permeability Measurements [27]

It should be noted that not all gases can be used in the bubble flowmeter. For example, high water-soluble gases such as ammonia

and hydrogen chloride will be dissolved in the soap solution, and this will cause a significant error in the reading [30].

Mass Flowmeter

In the mass flowmeter approach, the volume flowrate of the permeate will be measured by an electrical signal. It is more accurate compared to the bubble flowmeter as the stopwatch will not be needed and this can minimize the uncertainty. Thermal mass flowmeters are widely used, and they work

based on the thermal conductivity of the gas. The unit consists of a filament where its temperature is maximum when no gas is fed. When the gas enters the flowmeter, a drop in temperature will occur and this can be related to the volume of the gas (Figure 5).

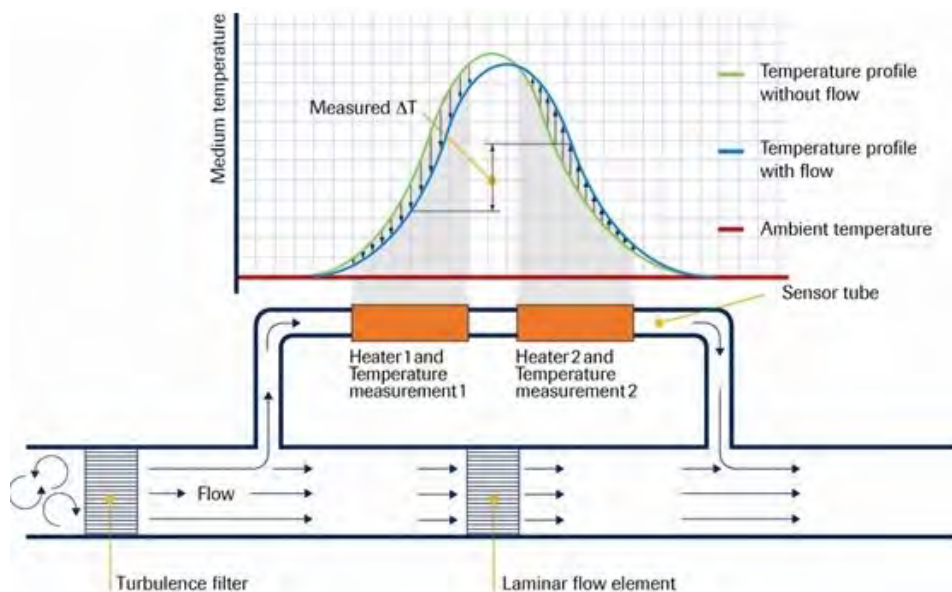


Figure 5. Operating Principle of the Thermal Mass Flowmeter [31]

It should be noted that the mass flowmeter is calibrated for specific gas and its accuracy is within $\pm 1\%$ [32]. However, using the same mass flowmeter for a different gas than the calibrated one may introduce an error in the measurement. For example, a calibrated mass flowmeter for nitrogen was tested for methane and the error reached 20.5% [33]. Yet, when the same mass flowmeter was used

for hydrogen, the error was only 1%. It was found that the error depends highly on the specific heat of the gas which is defined as the required energy to raise the gas temperature by 1 K of a unit mass of gas at constant pressure (C_p). Table 2 shows the calculated correction factor (CF) for a nitrogen-calibrated mass flowmeter tested with other gases. The correction factor was calculated using the following equation:

$$CF = \frac{V_A}{V_B} = \frac{(C_p M)_A}{(C_p M)_B} \quad (7)$$

where B is the tested gas and A is the calibrated gas. M is the molecular weight and C_p is the specific heat at constant pressure. So, if the mass flowmeter is calibrated with methane, and butane is to be used, equation 7 will give a correction factor of 0.37. The absolute average error of the previous equation is 3.1%.

The data in some mass flowmeters are given in NTP while the others are given in STP. To calculate the permeability in Barrer or GPU, the data of volume flowrate should be converted to STP using equation 3. The mass flowmeters are capable of reading flows from 0.0003 to 40,000 $\text{cm}^3 \text{s}^{-1}$ [34]. Furthermore, the technique can be used to monitor the membrane permeability for long-term operation.

Table 2. Correction Factor for the Conversion of a Nitrogen-calibrated Mass Flowmeter for Use with Other Gases [35]

Tested Gas	C_p (kJ kg ⁻¹ K ⁻¹)	M (g mol ⁻¹)	CF
Ammonia	2.19	17.03	0.78
Argon	0.52	39.95	1.40
Butane	1.67	58.12	0.30
Carbon dioxide	0.84	44.01	0.79
Ethane	1.75	30.07	0.55
Helium	5.19	4.02	1.40
Hydrogen	14.32	2.02	1.01
Methane	2.22	16.04	0.82
Nitrogen	1.04	28.02	1.00

Time-Lag Method

The time-lag method is based on a closed volume in which the permeate flowrate will cause an increase in the pressure with time. The volume of the closed system should be accurately determined taking into consideration the volume of pipes. Before the experiment, the system is vacuumed using a pump and a pressure gauge is utilized to monitor the pressure. The system should be leak-free otherwise, the permeability data

will be incorrect. To make sure the setup is gas-tight, the system is kept under vacuum (with no gas fed) for about 24 h. First, the vacuum pump should be run for about 30 min, and then the valve before the pump is closed. Generally, the pressure gauge should give a reading below 3 mbar for the system to be considered gas-tight. Figure 6 shows the setup for the time-lag experiment.

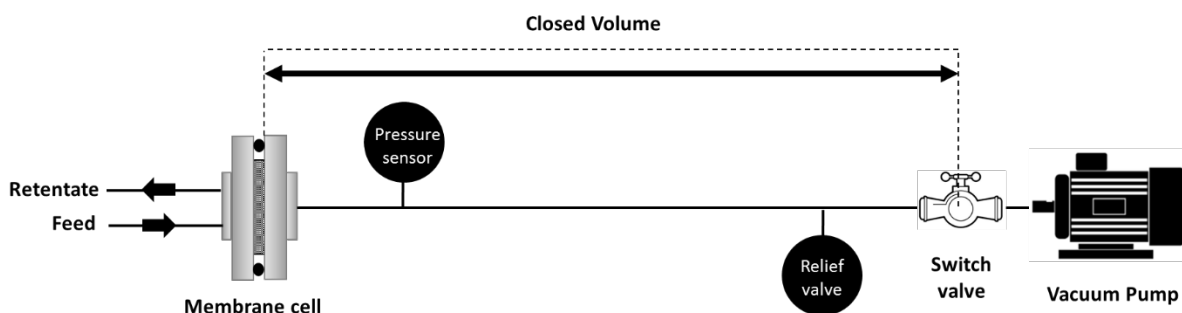


Figure 6. Experimental Setup for the Time-lag Method for Permeability Measurements [36]

After feeding the gas to the membrane, the permeated gas will cause a pressure buildup. The experiment is usually terminated when the pressure reaches 1 atm. Gauge-pressure

data should be monitored along with the time on stream. The time starts at 0 s when the gas is fed to the membrane. The permeability (in Barrer) can be then calculated using [37]:

$$P \text{ (Barrer)} = \frac{273}{76} \left[\frac{V_b \times l}{A \times T \times p_a} \right] \frac{dp_b}{dt} \times 10^{10} \quad (8)$$

where V_b is the volume of the closed system (cm^3), T is the temperature (K), p_a is the pressure of the feed gas (cmHg), and dp_b/dt is the rate of change of the pressure in the

permeate side with time (cmHg s^{-1}). The plot of the pressure in the permeate side along with time will give a straight-run and the slope is equal to dp_b/dt as given in Figure 7.

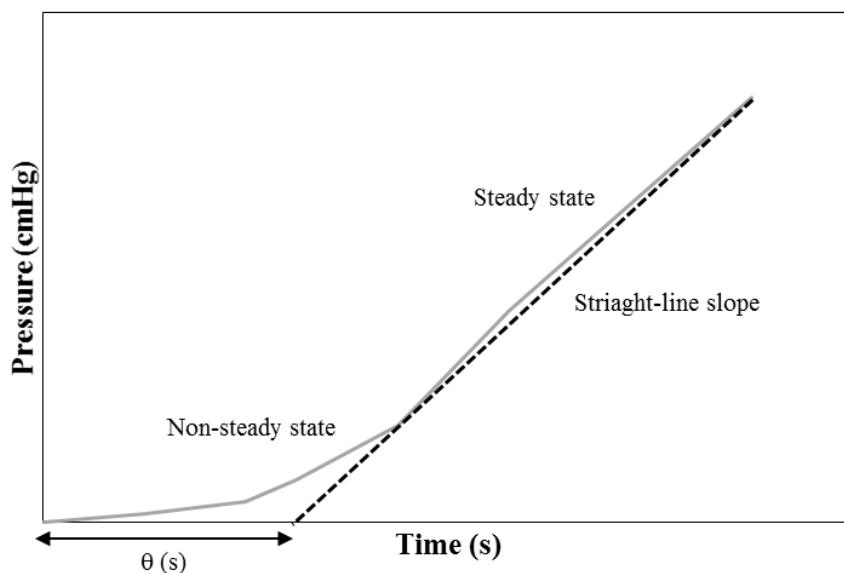


Figure 7. Plot of Pressure with Time in to Determine the Permeability and Diffusion and Solubility Coefficients [38]

For the first time of operation, it is expected to observe a non-steady-state line. After a certain time, a steady-state process is achieved and a straight slope line will be noticed which will be used to calculate dp_b/dt . The time-lag method is beneficial

over the bubble and mass flowmeters for very low permeate flowrates. Furthermore, the time-lag technique can be used to determine the diffusivity (or diffusion coefficient, D) by the following correlation [16]:

$$D \text{ (cm}^2 \text{ s}^{-1}\text{)} = \frac{l^2}{6\theta} \quad (9)$$

where l is the membrane thickness (cm) and θ is the time lag (s). The time lag is calculated based on the intercept of dp_b/dt line as

$$S[\text{cm}^3(\text{STP})\text{cm}^{-3}\text{cmHg}^{-1}] = \frac{P}{D} \quad (10)$$

where P is the permeability and D is the diffusion coefficient. The accuracy of the time-lag method can vary from 3 to 27% for permeability and diffusion/solubility coef-

shown in Figure 7. The solubility (K) can be then calculated from equation 1:

ficients [39]. Table 3 shows the advantages and limitations of bubble flowmeter, mass flowmeter, and the time-lag method for membrane permeability measurements.

Table 3. Comparison Between Different Techniques for Permeability Measurements in Membranes

Technique	Advantages	Limitations
Bubble Flowmeter	<ul style="list-style-type: none"> • Cost effective. • Good flowrate range. 	<ul style="list-style-type: none"> • Requires a stopwatch. • Some gases can dissolve in the soap solution.
Mass Flowmeter	<ul style="list-style-type: none"> • Wide flowrate range. • Long-term experiments 	<ul style="list-style-type: none"> • Use of a calibrated mass flowmeter for another gas may introduce error.
Time-lag	<ul style="list-style-type: none"> • Ability to measure very low flowrates. • Calculations of diffusion and solubility parameters. 	<ul style="list-style-type: none"> • Not suitable for high flowrates. • Volume of the closed system should be accurately measured.

3. Selectivity Calculations

To study the membrane performance, the membrane should be tested with at least two gases. This is because the membrane defects (such as voids and cracks) may result in an increase in the membrane permeability as there will be no flow resistance. This can be reflected if the selectivity is very low or

nearly 1. Usually, the permeability of gas a will be measured separately and then the permeability of gas b will be measured. Dividing the two permeabilities of gas a and b will give the ideal selectivity (α_{AB}):

$$\alpha_{AB} = \frac{P_A}{P_B} \quad (11)$$

where P_A is the permeability of gas a (the desired gas) and P_B is the permeability of gas b (the unwanted gas). Another way to calculate the selectivity is by introducing two or more gases at the same time. The user should define the gas mixture composition which is usually 50 vol% of gas a and 50 vol% of gas b . Because the permeate will have two or more gases, the produced gas should be analyzed to determine the composition so the

flowrate of each gas can be calculated. This is necessary so that the permeability of each gas can be determined. Usually, a gas-chromatography (GC) is used for this purpose but other instruments such as mass spectrometers, infrared analyzers, and colorimetric tubes can be implemented as well. After determining the volume percentage (vol%) of each gas, the volume flowrate of each gas in the permeate can be quantified by:

$$(V_P)_A = V_P \times (\text{vol}\%)_A \quad (12)$$

$$(V_P)_B = V_P \times (\text{vol}\%)_B \quad (13)$$

where V_P is the volume flowrate of the total gas in the permeate, $(V_P)_A$ is the volume flowrate of the product gas a , and $(V_P)_B$ is volume flowrate of gas b . The real selectivity can be then calculated using equation 11. Industrially, real selectivity is a must as it gives the actual membrane performance. The real selectivity can significantly change when mixtures are introduced compared to the ideal selectivity. For example, a cellulose acetate membrane was used for carbon di-

oxide separation from methane and the ideal selectivity was greatly reduced from 35 to 15 when a gas mixture was used [40]. It was also found that the real selectivity is a function of the composition of the mixture gas. Therefore, the ideal selectivity should be only used for research purposes and the real selectivity should be measured using actual feeds. Table 4 shows that the real selectivity is always lower than the ideal selectivity. Generally, the real selectivity is reduced by 10 to 63% compared to the ideal selectivity.

Table 4. Reduction in the Selectivity of Polymeric Membranes Due to the Use of Mixed Feeds

Gas separation	Ideal selectivity	Real selectivity	Reference
H ₂ /N ₂	281	250	[41]
H ₂ /CO ₂	4.5	3.6	[42]
CO ₂ /CH ₄	32–35	10–15	[40]
CO ₂ /N ₂	38	35	[43]
Propylene/propane	31	18	[44]

4. Calculations of Gas Recovery and Product Purity

In literature, the membrane performance is described by permeability and selectivity and these parameters are advantageous in comparing the membrane with other reported data. Furthermore, permeability and selectivity are useful for membrane modeling and upscaling. However, to evaluate the mem-

brane system with other gas-separation technologies such as amine scrubber and pressure swing adsorption (PSA), universal terms are preferred such as gas recovery and product purity. The following equation can be used then to calculate the gas recovery (R):

$$R(\%) = \frac{(V_P)_A}{(V_F)_A} \times 100 \quad (14)$$

where $(V_P)_A$ is the volume flowrate of gas a in the permeate and $(V_F)_A$ is the volume flowrate of the gas a in the feed. Normally, a commercial membrane is expected to have a recovery of 70 to 99%, depending on the separated gas [45]. For the product purity, mixed-gas experiments should be conducted and GC will determine the mol% of component a in the permeate. It should be noted

that the gas recovery and product purity greatly depend on the operating conditions such as feed composition, feed flowrate, pressure, temperature, and membrane area.

Product purity of a binary system can be still estimated from the data of ideal selectivity [46]. Mole balance across the membrane is applied by the following equation (neglecting accumulation):

$$x_F n_F = y_P n_P + x_R n_R \quad (15)$$

where n is the number of moles, x_F is the mole fraction of component a in the feed, x_R is the mole fraction in the retentate, and y_P is

the mole fraction in the product. Equation 15 can be rewritten as:

$$y_P n_P = x_F n_F - x_R n_R = QA(\overline{xP_F - yP_P}) \quad (16)$$

where Q is the permeance, A is the membrane area, and the last term is the trans-membrane pressure difference. P_F is the feed pressure while P_P is the permeate pressure. The trans-

membrane pressure difference can be simplified to (assuming complete mixing, neglecting radial gradients, constant pressures, and no mass-transfer resistance):

$$\overline{(xP_F - yP_P)} \cong x_F P_F - y_P P_P \quad (17)$$

The flux of component a (J_A) can be calculated by combining equations 16 and 17:

$$J_A = Q_A(x_F P_F - y_P P_P) \quad (18)$$

where Q_A , x_F and y_P are properties of component a. For component b, the flux is:

$$J_B = Q_B[(1 - x_F)P_F - (1 - y_P)P_P] \quad (19)$$

The ratio of absolute pressures (R) is defined as:

$$R = \frac{P_P}{P_F} \quad (20)$$

Now, equations 18 and 19 can be rewritten as:

$$J_A = Q_A P_F (x_F - y_P R) \quad (21)$$

$$J_B = Q_B P_F [(1 - x_F) - (1 - y_P)R] \quad (22)$$

The mole fraction of component a in the permeate can be estimated by:

$$y_P = \frac{J_A}{J_A + J_B} = \frac{Q_A P_F (x_F - y_P R)}{Q_A P_F (x_F - y_P R) + Q_B P_F [(1 - x_F) - (1 - y_P)R]} \quad (23)$$

Use of ideal selectivity in equation 11 but in terms of permeances gives:

$$\alpha = \frac{Q_A}{Q_B} \quad (24)$$

Applying the previous equation in equation 23 leads to:

$$y_P = \frac{J_A}{J_A + J_B} = \frac{(x_F - y_P R)}{(x_F - y_P R) + \frac{[(1 - x_F) - (1 - y_P)R]}{\alpha}} \quad (25)$$

The above equation can be rearranged resulting in a quadratic equation:

$$(\alpha - 1)y_p^2 + \left[1 - \alpha - \frac{1}{R} - \frac{x_F(\alpha - 1)}{R}\right]y_p + \frac{\alpha x_F}{R} = 0 \quad (26)$$

$$ay_p^2 + by_p + c = 0 \quad (27)$$

The solution for equation 27 is:

$$y_p = \frac{-b \pm \sqrt{b^2 - 4ac}}{2a} \quad (28)$$

So, to calculate the product purity for a binary system, the following data are needed: feed

and permeate pressures, feed composition, and ideal selectivity value.

5. Conclusions

The membrane is an energy-efficient technology for gas separation. It requires minimum supervision and has a long operating life. The membrane performance is determined by measuring the gas permeability and selectivity. However, the data can change significantly based on the experimental setup. Permeability is defined as the product of solubility and diffusivity, and it can be calculated based on measuring the flowrate of the permeate. The user should define the operating conditions before performing the experiment, which generally are: feed flowrate of 0.1–1 cm³ s⁻¹, temperature of 25–35°C, pressure of 3–10 bar, membrane effective area of 10–15 cm², and membrane thickness of 10–300 μm. There are mainly three ways to measure the permeate flowrate: bubble flowmeter, mass flowmeter, and time-lag method. The bubble flowmeter provides a low-cost solution for flowrates ranging from

0.1 to 1000 cm³ s⁻¹. The mass flowmeters are generally more accurate than the bubble flowmeters with a wider flow range. The time-lag method is useful for low flowrates, and it can be also used to determine the solubility and diffusion coefficients. The membrane should be tested for two or more gases to calculate the selectivity. If the gases were fed separately, this would give the ideal selectivity. However, for commercial applications, the mixed gas should be fed directly to the membrane and a gas chromatograph has to be used to determine the composition of the permeate. After that, the real selectivity can be stated. The real selectivity could vary significantly from the ideal selectivity, and this would seriously affect the membrane performance. To evaluate the membrane unit with other separation techniques, common terms are usually preferred such as gas recovery and product purity.

6. Funding

This research received no external funding.

7. Conflict of Interest

The authors declare no conflict of interest.

8. References

1. Baker R. Future directions of membrane gas separation technology. *Ind. Eng. Chem.*, 2002, 41, 1393-1411.
2. Henis J, Tripodi M. A novel approach to gas separations using composite hollow fiber membranes. *Sep. Sci. Technol.*, 1980, 15, 1059-1068.
3. Ismail A, Khulbe K, Matsuura T in *Gas Separation Membranes: Polymeric and Inorganic*, Springer International Publishing, US, 2015.
4. Ismail A, Matsuura T in *Sustainable Membrane Technology for Energy, Water, and Environment*, Wiley, 2012.
5. He X, Lie J, Sheridan E, Hägg M-B. CO₂ capture by hollow fibre carbon membranes: Experiments and process simulations. *Energy Procedia*, 2009, 1, 261-268.
6. Ball P. Scale-up and scale-down of membrane-based separation processes. *Membr. Technol.*, 2000, 2000, 10-13.
7. Wijmans J, Baker R. The solution-diffusion model: A review. *J. Membr. Sci.*, 1995, 107, 1-21.
8. Baker R in *Membrane Technology and Applications*, Wiley, 2012.
9. Lin L, Feng C, Lopez R, Coronell O. Identifying facile and accurate methods to measure the thickness of the active layers of thin-film composite membranes – A comparison of seven characterization techniques. *J. Membr. Sci.*, 2016, 498, 167-179.
10. Yang E, Goh K, Chuah C, Wang R, Bae T-H. Asymmetric mixed-matrix membranes incorporated with nitrogen-doped graphene nanosheets for highly selective gas separation. *J. Membr. Sci.*, 2020, 118293.
11. Marchese J, Pagliero C. Characterization of asymmetric polysulphone membranes for gas separation. *Gas Sep. Purif.*, 1991, 5, 215-221.
12. Matsuura T in *Synthetic Membranes and Membrane Separation Processes*, Taylor & Francis, 1993.
13. Scholes C, Chen G, Lu H, Kentish S. Crosslinked PEG and PEBAX membranes for concurrent permeation of water and carbon dioxide. *Membranes*, 2016, 6, 1.
14. Liu SL, Wang R, Liu Y, Chng M., Chung T. The physical and gas permeation properties of 6FDA-durene/2,6-diaminotoluene copolyimides. *Polymer*, 2001, 42, 8847-8855.
15. Basile A, Nunes S in *Advanced Membrane Science and Technology for Sustainable Energy and Environ-*

- mental Applications, Elsevier Science, 2011.
16. Koolivand H, Sharif A, Kashani M, Karimi M, Salooki M, Semsarzadeh M. Functionalized graphene oxide/polyimide nanocomposites as highly CO₂-selective membranes. *J. Polym. Res.*, 2014, 21, 599.
 17. Liu Y, Wang R, Chung T-S. Chemical cross-linking modification of polyimide membranes for gas separation. *J. Membr. Sci.*, 2001, 189, 231-239.
 18. Calle M, Lozano A, de Abajo J, de la Campa J, Álvarez C. Design of gas separation membranes derived of rigid aromatic polyimides. 1. Polymers from diamines containing di-tert-butyl side groups. *J. Membr. Sci.*, 2010, 365, 145-153.
 19. Espeso J, Lozano A, de la Campa J, de Abajo J. Effect of substituents on the permeation properties of polyamide membranes. *J. Membr. Sci.*, 2006, 280, 659-665.
 20. David O, Gorri D, Nijmeijer K, Ortiz I, Urriaga A. Hydrogen separation from multicomponent gas mixtures containing CO, N₂ and CO₂ using Matrimid® asymmetric hollow fiber membranes. *J. Membr. Sci.*, 2012, 419-420, 49-56.
 21. Vaughn J, Koros W. Effect of the amide bond diamine structure on the CO₂, H₂S, and CH₄ transport properties of a series of novel 6FDA-based polyamide-imides for natural gas purification. *Macromolecules*, 45, 7036-7049, 2012.
 22. Vaughn J, Koros W. Analysis of feed stream acid gas concentration effects on the transport properties and separation performance of polymeric membranes for natural gas sweetening: A comparison between a glassy and rubbery polymer. *J. Membr. Sci.*, 2014, 465, 107-116.
 23. Ren X., Ren J, Deng M. Poly(amide-6-b-ethylene oxide) membranes for sour gas separation. *Sep. Purif. Technol.*, 2012, 89, 1-8.
 24. Bernardo P, Drioli E, Golemme G. Membrane gas separation: A review/state of the art. *Ind. Eng. Chem. Res.*, 2009, 48, 4638-4663.
 25. Flaconnèche B, Martin J, Klopffer M. Permeability, diffusion and solubility of gases in polyethylene, polyamide 11 and poly(vinylidene fluoride). *Oil Gas Sci. Technol.*, 2001, 261-278.
 26. Scott K, Hughes R in *Industrial Membrane Separation Technology*, Springer Netherlands, 2012.
 27. Lashkari S, Kruczek B. Development of a fully automated soap flowmeter for micro flow measurements. *Flow Meas. Instrum.*, 2008, 19, 397-403.
 28. de Matos M, Rodrigues N. Gas mass-flow meters: Measurement and uncertainties. *Flow Meas. Instrum.*, 2013, 33, 45-54.
 29. Levy A. The accuracy of the bubble meter method for gas flow measurements. *J. Sci. Instrum.*, 1964, 41, 449-453.
 30. Nelson G in *Gas Mixtures: Preparation and Control*, CRC Press, 2018.
 31. Bronkhorst. [last accessed 3/04/2022] <https://www.bronkhorst.com/int/blog/good-to-know-thermal-mass-flow-sensor-bypass-versus-cta/>
 32. *Flowmeters for system applications designer checklist: Flow meter designer checklist*, Instrumentation Testing Association, 1999.
 33. Sahshi G, Mahendra A, Gouthaman G. Understanding the compatibility

- of thermal mass flow meter with various process gases. *J. Chem. Eng. Process Technol.*, 2012, S1, 1-7.
34. Bau H, DeRoos N, Kloeck B, Göpel W, Hesse J, Zemel J in *Sensors, Mechanical Sensors*, Wiley, 2008.
 35. Lide D in *Handbook of Chemistry and Physics*, CRC Press, US, 2004.
 36. Malagón-Romero D, Ladino A, Ortiz N, Green L. Characterization of a polymeric membrane for the separation of hydrogen in a mixture with CO₂. *Open Fuels Energy Sci. J.*, 2016, 9.
 37. Wu H, Thibault J, Kruczek B. The validity of the time-lag method for the characterization of mixed-matrix membranes. *J. Membr. Sci.*, 2021, 618, 118715.
 38. Ebadi A, Sanaeepur H, Kargari A, Moghadassi A. Direct determination of concentration-dependent diffusion coefficient in polymeric membranes based on the Frisch method. *Sep. Purif. Technol.*, 2011, 82, 102-113.
 39. Ye X, Lv L, Zhao X, Wang K. Permeation time lag in polymeric hollow fiber membranes. *J. Membr. Sci.*, 2006, 283, 425-429.
 40. Baker R, Low B. Gas separation membrane materials: A perspective. *Macromolecules*, 2014, 47, 6999-7013.
 41. Yáñez M, Ortiz A, Gorri D, Ortiz I. Comparative performance of commercial polymeric membranes in the recovery of industrial hydrogen waste gas streams. *Int. J. Hydrogen Energy*, 2020.
 42. Pesiri D, Jorgensen B, Dye R. Thermal optimization of polybenzimidazole meniscus membranes for the separation of hydrogen, methane, and carbon dioxide. *J. Membr. Sci.*, 2003, 218, 11-18.
 43. Xin Q, Ma F, Zhang L, Wang S, Li Y, Ye H, Ding X, Lin L, Zhang Y, Cao X. Interface engineering of mixed matrix membrane via CO₂-philic polymer brush functionalized graphene oxide nanosheets for efficient gas separation. *J. Membr. Sci.*, 2019, 586, 23-33.
 44. Zhang C, Dai Y, Johnson J, Karvan O, Koros W. High performance ZIF-8/6FDA-DAM mixed matrix membrane for propylene/propane separations. *J. Membr. Sci.*, 2012, 389, 34-42.
 45. Alqaheem Y, Alomair A, Vinoba M, Pérez A. Polymeric gas-separation membranes for petroleum refining. *Int. J. Polym. Sci.*, 2017, 1-19.
 46. McCabe W, Smith J, Harriott P in *Unit Operations of Chemical Engineering*, McGraw-Hill Education, 2005.